Front. Phys. 13(5), 130319 (2018)
https://doi.org/10.1007/s11467-018-0824-9

RESEARCH ARTICLE

Towards quantum entanglement of micromirrors via a two-level atom and radiation pressure

Zhi-Rong Zhong[1,†], **Xin Wang**[2], **Wei Qin**[3]

[1] *Fujian Key Laboratory of Quantum Information and Quantum Optics, College of Physics and Information Engineering, Fuzhou University, Fuzhou 350116, China*
[2] *Institute of Quantum Optics and Quantum Information, School of Science, Xi'an Jiaotong University, Xi'an 710049, China*
[3] *Quantum Physics and Quantum Information Division, Beijing Computational Science Research Center, Beijing 100193, China*
Corresponding authors. E-mail: [†]*zhirz@fzu.edu.cn*
Received February 25, 2018; accepted June 7, 2018

We propose a method to entangle two vibrating microsize mirrors (i.e., mechanical oscillators) in a cavity optomechanical system. In this scheme, we discuss both the resonant and large-detuning conditions, and show that the entanglement of two mechanical oscillators can be achieved with the assistance of a two-level atom and cavity-radiation pressure. In the resonant case, the operation time is relatively short, which is desirable to minimize the effects of decoherence. While in the large-detuning case, the cavity is only virtually excited during the interaction. Therefore, the decay of the cavity is effectively suppressed, which makes the efficient decoherence time of the cavity to be greatly prolonged. Thus, we observe that this virtual-photon process of *microscopic* objects may induce the entanglement of *macroscopic* objects. Moreover, in both cases, the generation of entanglement is deterministic and no measurements on the atom and the cavity are required. These are experimentally important. Finally, the decoherence effect and the experimental feasibility of the proposal are briefly discussed.

Keywords cavity optomechanical system, atomic, entanglement

PACS numbers 03.67.Bg, 31.30.J, 05.45.Xt, 42.50.Pq

1 Introduction

Quantum entanglement is one of the most intriguing phenomena in the quantum world. The investigation of entanglement is of interest both for fundamental tasks in quantum mechanics and for various applications in quantum-information processing (QIP) [1–6]. An exciting topic is the possibility of coherent manipulation (i.e., entanglement generation, quantum state transfer, and the construction of phase gates, etc.) of distinct macroscopic objects. This is still a great experimental challenge, because of the unavoidable decoherence and dissipation associated with such systems. The quest for entanglement generation of such macroscopic objects is not only motivated by their applications in testing the fundamentals of quantum mechanics and for the clarification of quantum-to-classical transition (i.e., the boundary between classical and quantum worlds), but also motivated by potential applications of quantum technologies, such as quantum metrology [7–9], high-precision measurements [10–12], as well as quantum interfaces [13, 14] for architectures of quantum information and quantum computing. Thus, much attention has been paid to the generation of this type of entanglement in the past decades [3, 15–25].

A promising venue to realize entanglement of macroscopic objects is provided by cavity-optomechanical systems, where a cavity field couples to a mechanical oscillator via the radiation-pressure force interaction [3]. Based on such systems, the entanglement between a mechanical oscillator and cavity modes [26–28], as well as between different mechanical oscillators [29–37] or different cavity modes [38–41], and a superposition state (a Schrödinger cat-like state) of a mirror [42] have been demonstrated or, at least, predicted in recent years.

In the above schemes, the generation of entanglement is typically achieved with the assistance of an extra

driving laser field. However, the atomic medium plays an important role in the interaction of cavity-quantum-electrodynamic (QED) system. Interesting phenomena should be revealed if an atom is trapped in a cavity-optomechanical system. Fortunately, many encouraging results, e.g., strong coupling between a single trapped atom and a mechanical oscillator [43–47], tripartite entanglement among an atom, a mechanical oscillator, and a cavity field [48], or long-distance coupling of an atomic ensemble to a micromechanical membrane [49–51] have recently been explored.

On the other hand, ground-state cooling [52–65] of mechanical oscillators has also been studied theoretically and demonstrated experimentally in cavity-optomechanical systems. As a result, many recent theoretical investigations focus on the single-photon strong-coupling regime [34, 66–73], in which the radiation pressure of a single photon can produce observable effects. In this regime, a strong photon nonlinearity at the few-photon level (resulting in, e.g., photon blockade) can be induced by the radiation-pressure coupling [73–77].

In this paper, we propose a scheme to entangle two mechanical oscillators with the assistance of a two-level atom and radiation pressure in a cavity-optomechanical system. Our proposal focuses on the single-photon strong-coupling regime. We show that, in a resonant regime, the radiation pressure induced by a photon created by the atom-cavity interaction can lead to the entanglement of two mechanical oscillators. In this case, the operation time is relatively short, which is desirable, to minimize the effects of decoherence. In the large-detuning regime, we show that a direct and effective coupling can be realized between two mechanical oscillators induced by the cavity mode and the atom. In this case, the cavity field is only virtually excited during the operation. Therefore, the decay of the cavity is effectively suppressed, which makes our proposal very robust against cavity decoherence, as we show by applying the master-equation approach. Moreover, in these two cases, the generation of entanglement is deterministic and *no* measurements on the atom and cavity are required. These are important advantages from the experimental point of view. As we show below, although the target entangled state of these two cases is similar, there are still two main differences between them. First, there are different physical mechanics leading to this entanglement. Secondly, the initial conditions of the system are different.

It is worth comparing our model with that reported in Ref. [29], where the entanglement of mechanical resonators was predicted in an optomechanical system with a classical drive without an atom. Note that in our proposal, we predict the entanglement of mechanical resonators in a hybrid optomechanical system with a two-level atom and without a classical drive. One can interpret the interaction between the atom and a cavity field, which is described by the Jaynes-Cummings model, as a kind of a quantum drive. In our proposal, we will show how to generate entanglement not only in resonant case but also in the large-detuning case. Moreover, in this large-detuning regime, we show, in contrast to the model of Ref. [29], that a direct effective coupling between the two mechanical resonators can be obtained.

2 Theoretical model and numerically simulation

Our proposal is based on a single-mode cavity with two movable perfectly-reflecting microsize mirrors (treated as mechanical oscillators), as sketched in Fig. 1(a). A two-level atom (with levels denoted as $|e\rangle$ and $|g\rangle$) is trapped in the cavity. The atomic transition $|e\rangle \longleftrightarrow |g\rangle$ couples the atom to the cavity mode. Also, the cavity mode couples to the mechanical oscillators through the radiation-pressure interaction. The total Hamiltonian of this system can be expressed in the form

$$H = H_0 + H_{\rm OM} + H_{\rm JC}, \tag{1}$$

where

$$H_0 = \hbar\omega_c a^\dagger a + \hbar\omega_e |e\rangle\langle e| + \hbar\omega_m \sum_{j=1,2} b_j^\dagger b_j \tag{2}$$

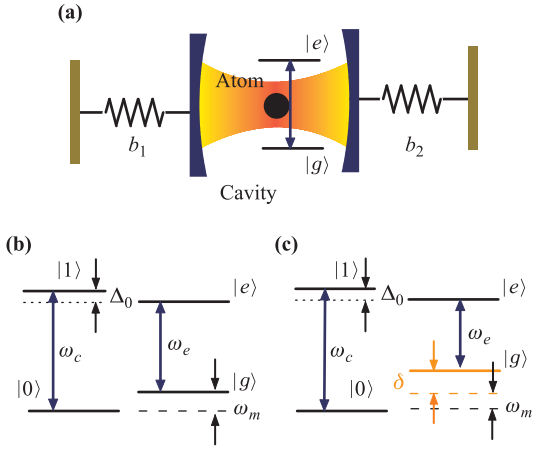

Fig. 1 **(a)** Schematic diagram of a cavity-optomechanical system. The cavity is formed by two moving micro- or nano-size mirrors, and contains a two-level atom with levels labeled as $|g\rangle$ and $|e\rangle$. The atomic transition $|e\rangle \leftrightarrow |g\rangle$ couples the atom to the cavity field and, simultaneously, the field couples to the mechanical oscillators through the radiation-pressure interaction. Energy levels for **(b)** the resonant ($\delta = 0$) and **(c)** with large-detuning ($\delta \gg 0$) interactions, where $\delta \equiv \omega_c - \omega_e - \Delta_0 + \omega_m$.

is the free Hamiltonian (assuming $\omega_g = 0$),

$$H_{\rm OM} = \hbar g_0 a^\dagger a \sum_{j=1,2} (b_j^\dagger + b_j) \tag{3}$$

is the standard optomechanical Hamiltonian, and

$$H_{\rm JC} = \hbar g (a|e\rangle\langle g| + a^\dagger |g\rangle\langle e|) \tag{4}$$

is the standard Jaynes-Cummings model under the rotating-wave approximation. Here a ($a^\dagger$) is the annihilation (creation) operator for the cavity, and b_j ($b_j^\dagger$) is the annihilation (creation) operator for the jth mechanical oscillator ($j = 1, 2$). The parameter ω_c is the frequency of the cavity, ω_m is the frequency of the mechanical oscillators (for simplicity, we here assume the two mechanical oscillators have the same frequency). Here ω_e is the atomic transition frequency ($|g\rangle$ is assumed to be the null-energy level), g_1 is the atom-cavity coupling strength. In addition, $g_0 = \omega_c x_{\rm zpf}/L$ is the single-photon optomechanical coupling strength, where $x_{\rm zpf} = \sqrt{1/(2M\omega_m)}$ is the zero-point fluctuation of the moving mirror with mass M, and L is the length of the cavity.

We first apply a unitary transformation $V_1 = \exp[i\omega_e(a^\dagger a + |e\rangle\langle e|)t]$ to the above Hamiltonian by using the standard formula $H_1 = V_1 H V_1^\dagger - {\rm i}\hbar V_1 \frac{\partial V_1^\dagger}{\partial t}$, which results in

$$H_1 = \hbar\Delta a^\dagger a + \hbar\omega_m \sum_{j=1,2} b_j^\dagger b_j + H_{\rm OM} + H_{\rm JC}, \tag{5}$$

where $\Delta = \omega_c - \omega_e$ is the detuning between the cavity frequency ω_c and the atomic-transition frequency ω_e. We now introduce another unitary operator $V_2 = \exp\left[(g_0/\omega_m)a^\dagger a \sum_{j=1,2}(b_j^\dagger - b_j)\right]$ to transform the Hamiltonian H_1 to $H_2 = V_2 H_1 V_2^\dagger$. Thus, we obtain

$$\begin{aligned} H_2 = {} & \hbar(\Delta - \Delta_0 a^\dagger a)a^\dagger a + \hbar\omega_m \sum_{j=1,2} b_j^\dagger b_j \\ & + \hbar g \left(a^\dagger |g\rangle\langle e| e^{\eta \sum_{j=1,2}(b_j^\dagger - b_j)} + H.c.\right), \end{aligned} \tag{6}$$

where $\Delta_0 = 2g_0^2/\omega_m$ characterizes the nonlinearity of the cavity field induced by mechanical oscillators. The parameter $\eta = g_0/\omega_m$ can be treated as the Lamb–Dicke parameter similar to that used in the analysis of trapped ions [78]. Let us now define a total excitation number operator of this system $\hat{N} = (a^+ a + |e\rangle\langle e|)$. As pointed out by Pirkkalainen *et al.* [45], the strong optomechanical coupling guarantees a big nonlinear parameter such that the photon blockade can occur. In this case, the cavity field is reduced to the two lowest-energy levels, $|0\rangle$ and $|1\rangle$. Then we can rewrite the creation operator of the cavity field as $a^\dagger = |1\rangle\langle 0| = \sigma_+$, and further introduce a new operator $\sigma_z = |1\rangle\langle 1| - |0\rangle\langle 0|$. Thus, the Hamiltonian H_2 can be rewritten as

$$H_2 = H_0^1 + H_i, \tag{7}$$

where

$$H_0^1 = \hbar\frac{\omega_0}{2}\sigma_z + \hbar\omega_m \sum_{j=1,2} b_j^\dagger b_j, \tag{8}$$

and

$$\begin{aligned} H_I' = {} & \hbar g \sigma_+ |g\rangle\langle e| \exp\left[\eta \sum_{j=1,2}(b_j^\dagger - b_j)\right] + H.c. \\ = {} & \hbar g \sigma_+ |g\rangle\langle e| e^{-\eta^2} \sum_{j=1,2} \sum_{i_1,i_2=1}^{n} \frac{(-1)^{i_2}\eta^{(i_1+i_2)}}{i_1! i_2!} b_j^{\dagger i_1} b_j^{i_2} + H.c. \end{aligned} \tag{9}$$

Here, $\omega_0 = \Delta - \Delta_0$. Considering the Lamb-Dicke approximation condition, $\eta = g_0/\omega_m \ll 1$, up to first order in η, the Hamiltonian in Eq. (9) becomes

$$H_I' = \hbar g \sigma_+ |g\rangle\langle e| \left[1 + \eta \sum_{j=1,2}(b_j^\dagger - b_j)\right] + H.c. \tag{10}$$

In the interaction picture, with $H_I = e^{{\rm i}H_0^1 t/\hbar} H_I' e^{-{\rm i}H_0^1 t/\hbar}$, we have a new Hamiltonian, which reads

$$\begin{aligned} H_I = {} & \hbar g \sigma_+ |g\rangle\langle e| \Big\{ \exp[{\rm i}(\Delta - \Delta_0)t] \\ & + \eta \sum_{j=1,2} (b_j^\dagger e^{{\rm i}\triangle_+ t} - b_j e^{-{\rm i}\triangle_- t}) \Big\} + H.c., \end{aligned} \tag{11}$$

where $\triangle_\pm = \omega_m \pm (\Delta - \Delta_0)$. In the following discussion, we will show how to utilize the Hamiltonian H_I to entangle two mechanical oscillator modes in two cases: the resonant and large-detuning regimes.

2.1 Resonant case

We begin our analysis by considering the resonant interaction. In this case, we set $\delta \equiv \Delta - \Delta_0 + \omega_m = 0$, and the corresponding level transitions are described in Fig. 1(b). If $\omega_m \gg g$, and thus $2\omega_m \gg g\eta$, we have a new Hamiltonian under the rotating-wave approximation,

$$H_I'' = \hbar\lambda \sigma_+ |g\rangle\langle e| (b_1^\dagger + b_2^\dagger) + H.c. \tag{12}$$

Here $\lambda = g\eta$ is the effective coupling coefficient. The above Hamiltonian shows that the $|e\rangle \longleftrightarrow |g\rangle$ transition of the atom will simultaneously create (annihilate) a photon and a phonon in two oscillators. According to this Hamiltonian, if the system is initially prepared in the state $|\Phi_0\rangle \equiv |e\rangle|0\rangle_c|0\rangle_{b1}|0\rangle_{b2}$, i.e., the atom is in the excited state, while the cavity field and the two mechanical oscillators are all in the vacuum state, the system will evolve within a subspace spanned by the states $\{|\Phi_0\rangle, |\Phi_1\rangle = |g\rangle|1\rangle_c|1\rangle_{b1}|0\rangle_{b2}, |\Phi_2\rangle = |g\rangle|1\rangle_c|0\rangle_{b1}|1\rangle_{b2}\}$.

With the initial state $|\Psi(t=0)\rangle = |\Phi_0\rangle$, the time evolution of the system is described by

$$|\Psi'(t)\rangle = \cos(\sqrt{2}\lambda t)|\Phi_0\rangle - \mathrm{i}\sin(\sqrt{2}\lambda t)|g\rangle|1\rangle_c|\Psi_+\rangle, \tag{13}$$

where $|\Psi_+\rangle = (1/\sqrt{2})(|1\rangle_{b1}|0\rangle_{b2} + |0\rangle_{b1}|1\rangle_{b2})$ is the "triplet" Bell state. Reversing the unitary transformation $V_2^\dagger$ on the state $|\Psi'(t)\rangle$, we obtain the final state

$$|\Psi(t)\rangle = \cos(\sqrt{2}\lambda t)|\Phi_0\rangle - \mathrm{i}\sin(\sqrt{2}\lambda t)D_{b_1}(\beta)D_{b_2}(\beta) \times|g\rangle|1\rangle_c|\Psi_+\rangle, \tag{14}$$

where $D_{b_j}(\beta) = \exp(\beta b_j^\dagger - \beta^* b_j)$ is the displacement operator with the parameter $\beta = -g_0 a^\dagger a/\omega_m$. If the interaction time is chosen as $\sqrt{2}\lambda t_1 = \pi/2$, the system evolves into

$$|\Psi(t_1)\rangle = D_{b_1}(\beta)D_{b_2}(\beta)|g\rangle|1\rangle_c|\Psi_+\rangle. \tag{15}$$

Where the minus sign and the imaginary part are absorbed in the common phase factor which has been discarded in the above equation. As seen from Eq. (15), the two mechanical oscillators are in maximally-entangled states, while the atom remains in its ground state and the cavity is in the one-photon state.

To confirm the validity of all our above derivations, we numerically simulate the dynamics governed by the effective model in Eq. (12) and compare it to the dynamics governed by the full Hamiltonian in Eq. (1). Defining the Lindblad-Kossakowski superoperator $D[o]\rho = (1/2)(2o\rho o^\dagger - o^\dagger o\rho - \rho o^\dagger o)$, the master equation for the system is given by

$$\dot{\rho} = -\mathrm{i}[H', \rho] + \kappa D[a]\rho + \gamma D[s]\rho + \gamma_1 \sum_{j=1}^{2} \left\{(n_{th}+1)D[b_j]\rho + n_{th}D[b_j^\dagger]\rho\right\}, \tag{16}$$

where $s = |g\rangle\langle e|$ is the atomic-transition operator, $H' = H$ and $H' = H_I$ correspond to the numerically-calculated full Hamiltonian in Eq. (1) and effective Hamiltonian in Eq. (12), respectively. Here we assume that the mechanical modes are coupled with a thermal reservoir with temperature T, and the corresponding thermal phonon number is $n_{th} = [\exp(\hbar\omega_m/k_B T) - 1]^{-1}$. The parameters κ, γ, and γ_1 are the cavity-decay rate, atomic spontaneous-emission rate, and the phonon-decay rate, respectively. Note that the numerical computation was performed using the Python package Qutip [79, 80]. We set the parameters as: $\Delta = 10g$, $\omega_m = 10.2g$, $g_0 = 0.2g$, and $\kappa = \gamma = \gamma_1 = 0.0005g$.

The validity of the effective model is numerically simulated by taking the evolution of the population $P = |\langle\psi_0|\psi(t)\rangle|^2$ of the state $|\psi_0\rangle = |e\rangle|0\rangle_c|0\rangle_{b1}|0\rangle_{b2}$ as an example, assuming the atom is initially in the excited state, the cavity mode and the two mechanical oscillators are all in the vacuum states.

Hereafter, we use the following compact notation for the states $|\psi_{\mathrm{dec}}(m_0m_1m_2)\rangle = |e\rangle|m_0\rangle_c|m_1\rangle_{b1}|m_2\rangle_{b2}$, where dec denotes the decimal representation of a number $(m_0m_1m_2)$, e.g., $|\psi_2\rangle = |e\rangle|0\rangle_c|1\rangle_{b1}|0\rangle_{b2}$. In Fig. 2, the red-dashed and blue-solid curves describe the time evolution of the population of state $|\psi\rangle$ governed by the effective and full Hamiltonians, respectively. It is obvious that the approximations, adopted when deriving the effective Hamiltonian, are valid, since the two curves described by the full and effective Hamiltonians nearly coincide.

The fidelity of the prepared entanglement is defined as $F = \langle\Psi(t_1)|\,\rho(t)\,|\Psi(t_1)\rangle$, where $\rho(t)$ is the density operator of the system, and $|\Psi(t_1)\rangle = D_{b_1}(\beta)D_{b_2}(\beta)|g\rangle|1\rangle_c|\Psi_+\rangle$ is the target maximally-entangled state for the two mechanical oscillators. For simplify, we first do not take the thermal phonons in the environment. The initial state of the system and the parameters are chosen to be the same as those in Fig. 2. In Fig. 3(a), the red-dashed and blue-solid curves describe the time evolution of the fidelity governed by the effective and full Hamiltonians, respectively. Figure 3(a) shows that the maximally-entangled state between the two mechanical oscillators with its fidelity higher than 0.94 (for the full Hamiltonian) and 0.96 (for the effective Hamiltonian) can be obtained at time $t_1 \simeq 55.8/g$. (The theoretical value is calculated based on $\sqrt{2}\lambda t_1 = \pi/2$, thus $t_1 \simeq 55.56/g$.) Thus, we can draw the following conclusion: that it is possible to significantly entangle two mechanical oscillators with the assistance of a two-level atom. Note that the generation of entanglement is deterministic and no measurements on the atom and

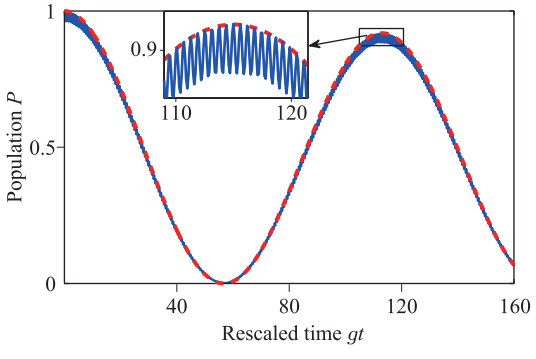

Fig. 2 ime evolution of the population $P = |\langle\psi_0|\psi(t)\rangle|^2$ governed respectively by the effective Hamiltonian (red-dashed curve) and the full Hamiltonian (blue-solid curve). We assume that the system is initially in the state $|\psi_0\rangle = |e\rangle|0_c\rangle|0_{b1}\rangle|0_{b2}\rangle$. The corresponding parameters are set to be: $\Delta = 10g$, $\omega_m = 10.2g$, $g_0 = 0.2g$, $n_{th} = 0$, and $\kappa = \gamma = \gamma_1 = 0.0005g$.

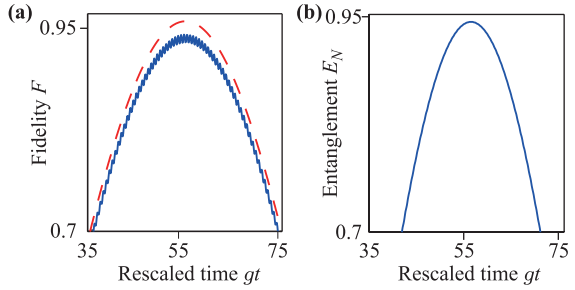

Fig. 3 **(a)** Time evolution of the fidelity F of the state $|\Psi(t_1)\rangle$, given by Eq. (15), governed by the effective Hamiltonian (red-dashed curve) and the full Hamiltonian (blue-solid curve), respectively, the system is initially in the state $|\psi_0\rangle = |e\rangle|0\rangle_c|0\rangle_{b1}|0\rangle_{b2}$. The maximally-entangled state between the two mechanical oscillators with fidelity higher than 0.94 (the full Hamiltonian) and 0.96 (the effective Hamiltonian) can be obtained at time $t_1 \simeq 55.8/g$ (our theoretical analysis predicts $t_1 \simeq 55.56/g$). **(b)** The time evolution of the entanglement of the mechanical oscillators, measured by the logarithmic negativity and governed by the full Hamiltonian. The entanglement can reach the value of 0.94 at time $t_1 \simeq 55.8/g$. The related parameters are set the same as those in Fig. 2.

cavity are required. These make the experimental setup simple, which is very important from the experimental point of view.

The entanglement of a mixed bipartite state ρ can be quantified by the so-called negativity [81],

$$N(\rho) = \frac{||\rho^\Gamma||_1 - 1}{2}, \tag{17}$$

where $||\rho^\Gamma||_1$ is the trace norm of the partially-transposed operator ρ^Γ. This definition of the negativity N can be rewritten in another equivalent form, as the absolute value of the sum of all the negative eigenvalues of ρ^Γ. Note that for two qubits, there might be at most one negative value.

Another closely-related entanglement measure is the logarithmic negativity, defined as [81]

$$E_N(\rho) = \log_2[2N(\rho) + 1] = ||\rho^\Gamma||_1, \tag{18}$$

which is applied in our numerical calculations. We note that $E_N(\rho) = 1$ for two-qubit Bell states. Both negativity and logarithmic negativity determine the degree of the nonpositivity of ρ^Γ and, thus, can be considered a quantitative version of the Peres-Horodecki separability criterion. More importantly, these measures are entanglement monotones and, thus, are useful in quantifying a degree of bipartite entanglement. We note that, although these measures are applicable to a bipartite state ρ of any dimension, these cannot detect nondistillable entanglement (i.e., bound entanglement) of systems more complex than two qubits, or a qubit and a qutrit [81]. The time evolution of this entanglement governed by the full Hamiltonian is plotted in Fig. 3(b), the parameters are set the same as those in Fig. 3(a). One can see from Fig. 3(b) that the entanglement between the two mechanical oscillators can reach the value of 0.94 at time $t_1 \simeq 55.8/g$.

In order to obtain more insight into the decoherence effect caused by the thermal noise, we now discuss the evolutions of master equation with different n_{th}. In Fig. 4(a), the green-solid, red-dashed, blue-dotted, and orange-dashed curves describe the time evolution of the fidelity governed by the full Hamiltonian under the condition that $n_{b_1} = n_{b_2} = 0.01$, $n_{b_1} = n_{b_2} = 0.1$, $n_{b_1} = n_{b_2} = 1$, and $n_{b_1} = n_{b_2} = 5$, respectively. Where n_{b_i} $(i = 1, 2)$ describe the initial thermal phonon. The system is initially in the state $|\psi_0\rangle = |e\rangle|0\rangle_c|0\rangle_{b1}|0\rangle_{b2}$, and the other parameters are set the same as those in Fig. (3). As we can see in Fig. (4)(a), when the initial thermal phonon is less than 1, the thermal phonon has less influence on the fidelity. But when the initial thermal phonon is more than 1. Moreover we show the highest fidelity changes with n_{th} in Fig. 4(b). It can be clearly found that the fidelity decreases rapidly when increasing of the thermal phonons. When $n_{th} = 2$, the highest fidelity decease to 0.84. Therefore, this proposal is more suitable for the case of low temperatures, i.e., near zero-temperature.

2.2 Large-detuning case

In this section, we consider the large-detuning regime, when $\delta = \Delta - \Delta_0 + \omega_m \gg 0$ in the Hamiltonian given in Eq. (11). The corresponding level transitions are described in Fig. 1(c). If the parameters are set to fulfill the conditions $\Delta - \Delta_0 \gg \max(\delta, g_1)$ and $\omega_m - \Delta + \Delta_0 \gg$

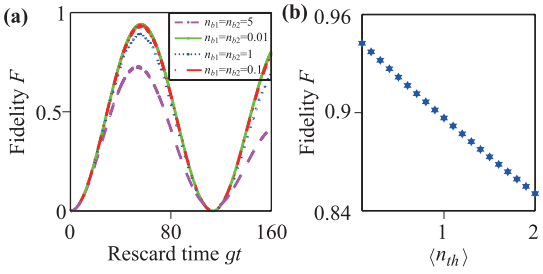

Fig. 4 **(a)** Time evolution of the fidelity F of the state $|\Psi(t_1)\rangle$ governed by the full Hamiltonian in a finite-temperature bath; the system is initially in the state $|\psi_0\rangle = |e\rangle|0\rangle_c|0\rangle_{b1}|0\rangle_{b2}$. The green-solid, red-dashed, blue-dotted and orange-dashed curves describe the time evolution of the fidelity governed by the full Hamiltonian under the condition that $n_{b_1} = n_{b_2} = 0.01$, $n_{b_1} = n_{b_2} = 0.1$, $n_{b_1} = n_{b_2} = 1$, and $n_{b_1} = n_{b_2} = 5$, respectively. **(b)** The highest fidelity F with different n_{th}. The highest fidelity decease to 0.84 when $n_{th} = 2$.

$\max(\delta, g_1\eta)$, under the rotating-wave approximation, the Hamiltonian in Eq. (11) can be rewritten as

$$H_e' = \hbar\lambda\sigma_+|g\rangle\langle e|\mathrm{e}^{-\mathrm{i}\delta t}(b_1^\dagger + b_2^\dagger) + H.c., \tag{19}$$

where $\lambda = g\eta$. In the case $\delta \gg \lambda$, there is no energy exchange between the atomic system and the cavity. Then the effective Hamiltonian is given by

$$\begin{aligned} H_e = \hbar\chi\big[&a^\dagger a|g\rangle\langle g|(b_1^\dagger b_1 + b_2^\dagger b_2) - aa^\dagger|e\rangle\langle e|(b_1^\dagger b_1 + b_2^\dagger b_2) \\ &+ (a^\dagger a|g\rangle\langle g| - aa^\dagger|e\rangle\langle e|)(b_1^\dagger b_2 + b_2^\dagger b_1)\big], \end{aligned} \tag{20}$$

where $\chi = \lambda^2/\delta$ is the effective coupling coefficient. In Eq. (20), the first and second terms describe the Stark shifts induced by the atom, cavity, and mechanical oscillators, while the third term describes the effective coupling between the two mechanical oscillators induced by the cavity mode and the atom. By considering a single-phonon condition, the interaction between the two mechanical oscillators is similar to the dipole interaction in atomic systems. Moreover, in this interaction, the cavity and atom act just as a medium, e.g., the cavity is only virtually excited and does not exchange energy with the atom during the operation, which is similar to the virtual-photon process in cavity-QED systems [82]. This is an interesting phenomenon, where the virtual-photon process of microscopic objects may induce the entanglement of macroscopic objects. This will help us to deeply look inside the clarification of quantum to classical transition [83]. If we assume the cavity field is initially in the vacuum state and the atom in the excited state, the Hamiltonian reduces to

$$H_e = -\hbar\chi|e\rangle\langle e|\big[(b_1^\dagger b_1 + b_2^\dagger b_2) + (b_1^\dagger b_2 + b_2^\dagger b_1)\big]. \tag{21}$$

The above Hamiltonian describes the effective coupling between the two mechanical oscillators. Although the Hamiltonian is similar to that reported by Buchmann *et al.* [84], the difference between them is obvious. Firstly, in our proposal, the effective coupling between the two mechanical oscillators is induced by the cavity mode and the atom, while the scheme in Ref. [84] is induced by a time-dependent cavity field. Moreover, our system works in the strong-coupling regime, while another scheme works in weak-coupling regime. Assume the system is initially in the state $|\psi_2\rangle = |e\rangle|0\rangle_c|1\rangle_{b1}|0\rangle_{b2}$, i.e., the atom is in the excited state, the cavity is in the vacuum state, and one of the mechanical oscillator modes is in one phonon state and the other in the vacuum state. Then, the state evolution of the system is given by

$$|\psi_2\rangle \to \exp(-2\mathrm{i}\chi t)\left[\cos(\chi t)|\psi_2\rangle - \mathrm{i}\sin(\chi t)|\psi_1\rangle\right]. \tag{22}$$

With the choice $\chi t' = \pi/4$, the system evolves to

$$|\Psi(t')\rangle = |e\rangle|0_c\rangle|\psi_B\rangle, \tag{23}$$

where $|\psi_B\rangle = (1/\sqrt{2})(|1\rangle_{b1}|0\rangle_{b2} - i|0\rangle_{b1}|1\rangle_{b2})$ is a Bell-like state, and we have discarded the common phase factor. In this situation, the two mechanical oscillators are in the maximally-entangled state, while the atom remains in the excited state and the cavity is in the vacuum state. Similar to the resonant case, the generation of entanglement is also deterministic and any measurements on the atom and cavity are not required. Notice that this idea can also be used to realize other quantum-information processing, e.g. quantum teleportation [85], construction of phase gates [1], or quantum-state transfer [86], etc.

The validity of all our above derivations is confirmed by comparing the numerically simulation of the dynamics governed by the effective model in Eq. (21) with the dynamics governed by the full Hamiltonian in Eq. (1). In this case, the master equation for the density matrix operator is also described in Eq. (16). The corresponding parameters are set as $\Delta = 10g$, $\omega_m = 10.6g$, $g_0 = 0.8g$, $n_{th} = 0$, and $\kappa = \gamma = \gamma_1 = 0.0001g$. In Fig. 5, the red-dash (magenta-dash) and blue-solid (green-solid) curves describe the time evolution of the population of the state $|\psi_2\rangle = |e\rangle|0\rangle_c|1\rangle_{b1}|0\rangle_{b2}$ ($|\psi_1\rangle = |e\rangle|0\rangle_c|0\rangle_{b1}|1\rangle_{b2}$) governed by the effective and full Hamiltonians, respectively. The system is initially in the state $|\psi_2\rangle$. We can see from Fig. 5 that the effective model is valid, since the numerical results governed by the effective Hamiltonian agree well with those for the full Hamiltonian. The black-solid (cyan-solid) curves in Fig. 5 describe the time evolution of the population of the state $|\psi_3\rangle = |g\rangle|1\rangle_c|1\rangle_{b1}|0\rangle_{b2}$ governed by the full Hamiltonian (the effective Hamiltonian). One can also see from Fig. 5 that the population of $|\psi_3\rangle$ is zero under the effective Hamiltonian and is less than 0.1 under the full Hamiltonian. This indicates that the cavity mode is hardly excited during the interaction.

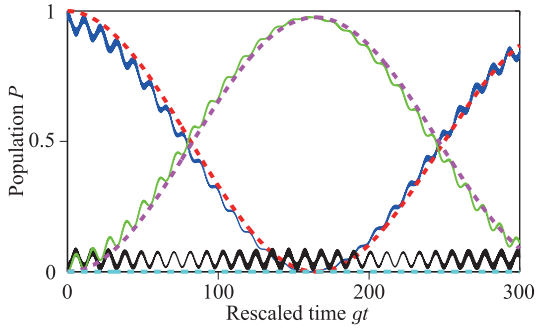

Fig. 5 The time evolution of the populations. The red-dash (magenta-dash) and the blue-solid (green-solid) curves describe the time evolution of the population $P = |\langle\psi_i|\psi(t)\rangle|^2$ of the state $|\psi_2\rangle = |e\rangle|0\rangle_c|1\rangle_{b1}|0\rangle_{b2}$ ($|\psi_1\rangle = |e\rangle|0\rangle_c|0\rangle_{b1}|1\rangle_{b2}$) governed by the effective and full Hamiltonians, respectively. The black-solid (cyan-solid) curves describe the time evolution of the population of the state $|\psi_3\rangle = |g\rangle|1_c\rangle|1_{b1}\rangle|0_{b2}\rangle$ governed by the full Hamiltonian (effective Hamiltonian). The system is initially in the state $|\psi_2\rangle = |e\rangle|0\rangle_c|1\rangle_{b1}|0\rangle_{b2}$ and the corresponding parameters are set to be: $\Delta = 10g$, $\omega_m = 10.6g$, $g_0 = 0.8g$, $n_{th} = 0$, and $\kappa = \gamma = \gamma_1 = 0.0001g$.

This is due to the fact that the effective atom-cavity interaction is nonresonant. As seen from the parameters used in the simulation, the detuning between ω_c and ω_e is much larger than the effective coupling constant χ.

In Fig. 6(a), the optimal fidelity of the target state $|\Psi\rangle = |e\rangle|0\rangle_c|\psi_B\rangle$ is plotted versus time with the same initial state and parameters as those used in Fig. 5. The corresponding fidelity is defined as $F = \langle\Psi|\,\rho(t)\,|\Psi\rangle$, where $\rho(t)$ is the density operator of the system. One can see from Fig. 6(a) that the maximum fidelity of the entangled state between the two mechanical oscillators is 0.95 (for the full Hamiltonian) and 0.98 (for the effective Hamiltonian) can be obtained at the time $t' \simeq 80.1/g$. The time evolutions of the entanglement governed by the full Hamiltonian is plotted in Fig. 6(b). As shown in Fig. 6(b), the entanglement between the two mechanical oscillators can reach the value of 0.95 at time $t_1 \simeq 80.1/g$. Thus, we conclude that the entanglement of the two mechanical oscillators is obtained by a virtual photon process. Moreover, during the operation, the cavity is hardly populated, and, thus the effective decoherence time of the cavity is greatly prolonged. However, due to the weak coupling, with a longer Rabi oscillation period, the decoherence effectively caused by the atomic spontaneous emission and phonon decay has a great influence on the fidelity of the target entangled state in the large-detuning case.

We also find that if $g = 0$ and the cavity is initially in the vacuum state then the entanglement between the mechanical modes b_1 and b_2 is always zero. But if $g = 0$ and the cavity is initially in the single-photon state $|1\rangle$, then the entanglement between the mechanical modes is nonzero, but still very small for short evolution times and increases very slowly with time. For these initial conditions, for example, the logarithmic negativity is equal to $E_N \simeq 1.8 \times 10^{-4}$ for $t = 160/g$ and $E_N \simeq 2.4 \times 10^{-4}$ for $t = 400/g$. This example shows the main advantage of our model with a two-level atom coupled to the cavity field (i.e., with $g \neq 0$) for the effective generation of highly-entangled states even for short evolution times.

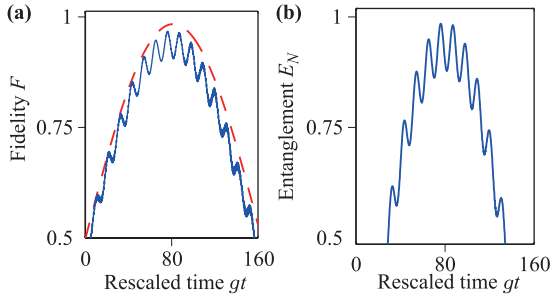

Fig. 6 **(a)** The time evolution of the fidelity of the target state $|\Psi\rangle = |e\rangle|0_c\rangle|\psi_B\rangle$ governed, respectively, by the effective Hamiltonian (red-dashed curve) and full Hamiltonian (blue-solid curve), when the system is initially in the state $|\psi_2\rangle = |e\rangle|0\rangle_c|1\rangle_{b1}|0\rangle_{b2}$. The maximally-entangled state between the two mechanical oscillators with fidelity higher than 0.95 (0.98) can be obtained at time $t' \simeq 80.1/g$ under the full Hamiltonian (effective Hamiltonian). **(b)** The time evolution of the entanglement of the mechanical oscillators as measured by the logarithmic negativity and governed by the full Hamiltonian. The entanglement can reach the value of 0.95 at time $t_1 \simeq 80.1/g$. The parameters are set the same as those in Fig. 5.

In order to obtain more insight into the decoherence effect caused by the cavity, atom, and mechanical oscillators, we discuss the fidelity of the entanglement state $|\Psi\rangle$ versus the cavity-decay rate κ, the atomic spontaneous-emission rate γ, and the phonon-decay rate γ_1 governed by the full Hamiltonian. In Fig. 7(a), we discuss the fidelity of the entangled state $|\Psi\rangle$ versus the cavity-decay rate and the atomic spontaneous-emission rate when assuming that the system is initially in the state $|\psi_2\rangle = |e\rangle|0\rangle_c|1\rangle_{b1}|0\rangle_{b2}$. The parameters we use here are $\Delta = 10g$, $\omega_m = 10.6g$, $g_0 = 0.8g$, $n_{th} = 0$, and $\gamma_1 = 0$. As seen from Fig. 7(a), the fidelity decreases when increasing the parameters γ and κ. In addition, one can see from Fig. 7(a) that the atomic spontaneous emission has stronger influence on the fidelity than the cavity decay. This is due to the fact that the cavity is hardly excited during the operation; thus, the decoherence caused by the cavity can be effectively suppressed. The atom is still in the excited state during the operation; thus, the atomic spontaneous emission has greater influence on the fidelity than that caused by the cavity decay. In Fig. 7(b), we show the fidelity of the target entangled state $|\Psi\rangle$ versus the phonon-decay rate γ_1 and the atomic spontaneous-emission rate γ with the same initial state used in Fig. 7(a). The others parameters used here are: $\Delta = 10g$, $\omega_m = 10.6g$, $g_0 = 0.8g$, $n_{th} = 0$, and $\kappa = 0$. As seen from Fig. 7(b), the decay of the phonon and the spontaneous emission of the atom both have great influence on the fidelity. The fidelity decreases quickly

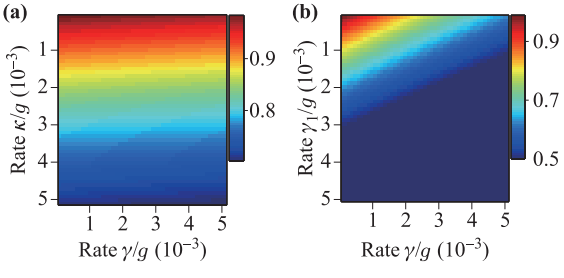

Fig. 7 The fidelity $F = \langle\Psi|\,\rho(t)\,|\Psi\rangle$ of the state $|\Psi\rangle = |e\rangle|0\rangle_c|\psi_B\rangle$ governed by the full Hamiltonian, versus the cavity decay rate κ, atomic spontaneous emission rate γ, and phonon decay rate γ_1. The system is initially in the state $|\psi_2\rangle = |e\rangle|0\rangle_c|1\rangle_{b1}|0\rangle_{b2}$. We set $\Delta = 10g$, $\omega_m = 10.6g$, $g_0 = 0.8g$, $n_{th} = 0$, $\gamma_1 = 0$ [Fig. 7(a)], and $\kappa = 0$ [Fig. 7(b)].

when increasing γ and γ_1. This is due to the fact that the phonon and atom are effectively populated during the operation.

3 Discussion and conclusions

It is useful to present a brief discussion of the experimental feasibility of the proposed model. (i) In order to achieve the target entangled state, the system should work in the single-photon strong-coupling regime, which requires that the single-photon coupling strength g_0 is much lager than the decay rates of the cavity field, the atomic spontaneous emission rate, and the phonon decay rate, i.e., $g_0 \gg \max(\kappa, \gamma, \gamma_1)$. (ii) The system should work in the deep-resolved sideband regime, which requires the frequency of the vibrational mode of the mechanical oscillators to be much lager than the decay rate of the cavity field, i.e., $\omega_m \gg \kappa$. As reported by Chan et al.[61], the frequency ω_m of a mechanical resonator formed in a silicon microchip can reach $\omega_m = 2\pi \times 3.9 \times 10^9$ Hz, the corresponding coupling coefficient is $g_o = 2\pi \times 9 \times 10^5$ Hz, and the decay rate of the cavity field is $\kappa = 2\pi \times 10^8$ Hz. Thus, the proposed proposal may be realized in optomechanical devices form by photonic crystal Nano beam. (iii) Noted that the target entanglement states are rely in the initial state of the system. Thus, it is necessary to discuss how to prepare the initial state of the system. In resonant condition, the initial state of the system is in the state $|\Phi_0\rangle \equiv |e\rangle|0\rangle_c|0\rangle_{b1}|0\rangle_{b2}$, which requires the two mechanical mirrors should be cooled to their ground states, this can be realized by the ground-state cooling method. While the initial state of the atom and the cavity can be prepared by the cavity QED method. In Large-detuning case, the system is initially in the state $|\psi_2\rangle = |e\rangle|0\rangle_c|1\rangle_{b1}|0\rangle_{b2}$, which requires one of the mechanical mirrors should be cooled to the ground state, and the other is in the one phonon state. Similarly to the resonant case, the initial state of the atom and the cavity can be prepared by the cavity QED method, and the ground state of the mechanical mirrors can be obtained by ground-state cooling method. While the one phonon of mechanical mirrors can be obtained by some theoretical schemes [34–36].

The difference between these two cases should be mentioned again. As we have seen, although the target entangled state for these two cases is similar, there are still two differences between them.

(i) The physical mechanism and the results induced by them are different. In our proposal, we discuss the resonant and large-detuning cases. For the resonant case, the operation time is relatively short, which is very desirable to minimize decoherence effects. However, in this case, the cavity mode is effectively populated during the operation, which reduces the decoherence time of the cavity. While in the large-detuning case, the cavity is hardly populated and, thus, the efficient decoherence time of the cavity is greatly prolonged. However, due to the weak coupling, the operation time is longer than the resonant case; thus, the decoherence effectively caused by the atomic spontaneou emission and phonon decay have considerable influence on the fidelity of the target entangled state in this case.

(ii) The initial states of the system are different. In the resonant case, the initial state is $|\psi_0\rangle = |e\rangle|0\rangle_c|0\rangle_{b1}|0\rangle_{b2}$, i.e., the atom is in the excited state, while the cavity mode and the mechanical oscillator modes are all in the vacuum state. While in the large-detuning case, the initial state is $|\psi_2\rangle = |e\rangle|0\rangle_c|1\rangle_{b1}|0\rangle_{b2}$, which requires the atom to be in the excited state, the cavity to be in the vacuum state, while one of the mechanical oscillator modes must be in the one-phonon state and the other in the vacuum state.

A possible measurement for the verification of entanglement should be considered. For resonant case, the measurement of the entanglement of mechanical oscillators can be achieved by the measurement the cavity field. The measurement of the cavity-field states can be realized using atom. Assuming that an atom in the ground state is flying through the cavity. If the atom is measured in the excited state, then the cavity is in a single-photon state and two mechanical oscillators are in the entanglement state. Similarly, for large-detuning case, the measurement of the entanglement of mechanical oscillators can also be achieved by the measurement the cavity field and the atom.

In conclusion, we have proposed a scheme to generate the entanglement of two vibrating micro-size mirrors (treated as mechanical oscillators) with the assistance of a two-level atom and radiation pressure in a cavity-optomechanical system. In the single-photon strong-coupling regime, the entanglement of the two mechanical oscillators is obtained through the radiation pressure induced by a photon which is emitted from the atom. We show that in a resonant case, the generation of entanglement is relatively rapid, which is significant in view of decoherence. While in the large-detuning case, the cavity is only virtually excited during the operation. This is an interesting phenomenon where the virtual photon process of microscopic objects may induce the entanglement of macroscopic objects. Therefore, the decay of the cavity is effectively suppressed, which makes the case robust against the cavity decoherence. Moreover, in the proposal, the entanglement generation is deterministic and any measurement on the system is unnecessary. This makes the proposed scheme simple and feasible. In addition, the decoherence effect and experimental feasibility of the proposal are briefly discussed. With the rapid im-

provement of the experimental techniques, this proposal may be realized in the near future.

Acknowledgements This work was supported by the National Natural Science Foundation of China under Grant Nos. 11674060, 11404061, and 11705030, the Natural Science Foundation of Fujian Province under Grant No. 2016J01018, and the Fujian Provincial Department of Education under Grant No. JZ160422.

References

1. M. A. Nielsen and I. L. Chuang, Quantum Computation and Quantum Information, Cambridge University Press, Cambridge, 2010
2. I. Buluta, S. Ashhab, and F. Nori, Natural and artificial atoms for quantum computation, *Rep. Prog. Phys.* 74(10), 104401 (2011)
3. M. Aspelmeyer, T. J. Kippenberg, and F. Marquardt, Cavity optomechanics, *Rev. Mod. Phys.* 86(4), 1391 (2014)
4. I. M. Georgescu, S. Ashhab, and F. Nori, Quantum simulation, *Rev. Mod. Phys.* 86(1), 153 (2014)
5. Z. L. Xiang, S. Ashhab, J. Q. You, and F. Nori, Hybrid quantum circuits: Superconducting circuits interacting with other quantum systems, *Rev. Mod. Phys.* 85(2), 623 (2013)
6. W. Qin, A. Miranowicz, P. B. Li, X.Y. Lü, J. Q. You, and F. Nori, Exponentially enhanced light-matter interaction, cooperativities, and steady-state entanglement using parametric amplification, *Rev. Lett.* 120(9), 093601 (2018)
7. V. Giovannetti, S. Lloyd, and L. Maccone, Quantum metrology, *Phys. Rev. Lett.* 96(1), 010401 (2006)
8. V. Giovannetti, S. Lloyd, and L. Maccone, Advances in quantum metrology, *Nat. Photonics* 5(4), 222 (2011)
9. J. B. Clark, F. Lecocq, R. W. Simmonds, J. Aumentado, and J. D. Teufel, Observation of strong radiation pressure forces from squeezed light on a mechanical oscillator, *Nat. Phys.* 12(7), 683 (2016)
10. K. Goda, O. Miyakawa, E. E. Mikhailov, S. Saraf, R. Adhikari, K. McKenzie, R. Ward, S. Vass, A. J. Weinstein, and N. Mavalvala, A quantum-enhanced prototype gravitational-wave detector, *Nat. Phys.* 4(6), 472 (2008)
11. U. B. Hoff, G. I. Harris, L. S. Madsen, H. Kerdoncuff, M. Lassen, B. M. Nielsen, W. P. Bowen, and U. L. Andersen, Quantum-enhanced micromechanical displacement sensitivity, *Opt. Lett.* 38(9), 1413 (2013)
12. R. C. Pooser and B. Lawrie, Ultrasensitive measurement of microcantilever displacement below the shot-noise limit, *Optica* 2(5), 393 (2015)
13. C. M. Caves, Quantum-mechanical noise in an interferometer, *Phys. Rev. D* 23(8), 1693 (1981)
14. D. Kienzler, C. Flühmann, V. Negnevitsky, H. Y. Lo, M. Marinelli, D. Nadlinger, and J. P. Home, Observation of quantum interference between separated mechanical oscillator wave packets, *Phys. Rev. Lett.* 116(14), 140402 (2016)
15. S. Mancini, V. Giovannetti, D. Vitali, and P. Tombesi, Entangling macroscopic oscillators exploiting radiation pressure, *Phys. Rev. Lett.* 88(12), 120401 (2002)
16. K. J. Vahala, Optical microcavities, *Nature* 424(6950), 839 (2003)
17. J. Eisert, M. B. Plenio, S. Bose, and J. Hartley, Towards quantum entanglement in nanoelectromechanical devices, *Phys. Rev. Lett.* 93(19), 190402 (2004)
18. X. B. Yan, W. Z. Jia, Y. Li, J. H. Wu, X. L. Li, and H. W. Mu, Optomechanically induced amplification and perfect transparency in double-cavity optomechanics, *Front. Phys.* 10(3), 351 (2015)
19. J. D. Jost, J. P. Home, J. M. Amini, D. Hanneke, R. Ozeri, C. Langer, J. J. Bollinger, D. Leibfried, and D. J. Wineland, Entangled mechanical oscillators, *Nature* 459(7247), 683 (2009)
20. Y. W. Hu, Y. F. Xiao, Y. C. Liu, and Q. Gong, Optomechanical sensing with on-chip microcavities, *Front. Phys.* 8(5), 475 (2013)
21. J. Q. Liao and L. Tian, Macroscopic quantum superposition in cavity optomechanics, *Phys. Rev. Lett.* 116(16), 163602 (2016)
22. C. F. Ockeloen-Korppi, E. Damskägg, J. M. Pirkkalainen, M. Asjad, A. Clerk, A. Massel, M. J. Woolley, and M. A. Sillanpää, Stabilized entanglement of massive mechanical oscillators, *Nature* 556(7702), 478 (2018)
23. R. Riedinger, A. Wallucks, I. Marinković, C. Löschnauer, M. Aspelmeyer, S. Hong, and S. Gröblacher, Remote quantum entanglement between two micromechanical oscillators, *Nature* 556(7702), 473 (2018)
24. C. G. Liao, R. X. Chen, X. Hong, and X. M. Lin, Reservoir-engineered entanglement in a hybrid modulated three-mode optomechanical system, *Phys. Rev. A* 97(4), 042314 (2018)
25. R. X. Chen, C. G. Liao, and X. M. Lin, Dissipative generation of significant amount of mechanical entanglement in a coupled optomechanical system, *Sci. Rep.* 7(1), 14497 (2017)
26. Q. Lin, B. He, R. Ghobadi, and C. Simon, Fully quantum approach to optomechanical entanglement, *Phys. Rev. A* 90(2), 022309 (2014)
27. E. Verhagen, S. Deleglise, S. Weis, A. Schliesser, and T. J. Kippenberg, Quantum-coherent coupling of a mechanical oscillator to an optical cavity mode, *Nature* 482(7383), 63 (2012)
28. T. A. Palomaki, J. D. Teufel, R. W. Simmonds, and K. W. Lehnert, Entangling mechanical motion with microwave fields, *Science* 342(6159), 710 (2013)

29. M. J. Hartmann and M. B. Plenio, Steady state entanglement in the mechanical vibrations of two dielectric membranes, *Phys. Rev. Lett.* 101(20), 200503 (2008)
30. C. Joshi, J. Larson, M. Jonson, E. Andersson, and P. Öhberg, Entanglement of distant optomechanical systems, *Phys. Rev. A* 85(3), 033805 (2012)
31. Y. D. Wang and A. A. Clerk, Reservoir-engineered entanglement in optomechanical systems, *Phys. Rev. Lett.* 110(25), 253601 (2013)
32. C. J. Yang, J. H. An, W. L. Yang, and Y. Li, Generation of stable entanglement between two cavity mirrors by squeezed-reservoir engineering, *Phys. Rev. A* 92(6), 062311 (2015)
33. H. Flayac, M. Minkov, and V. Savona, Remote macroscopic entanglement on a photonic crystal architecture, *Phys. Rev. A* 92(4), 043812 (2015)
34. J. Q. Liao, Q. Q. Wu, and F. Nori, Entangling two macroscopic mechanical mirrors in a two-cavity optomechanical system, *Phys. Rev. A* 89(1), 014302 (2014)
35. R. X. Chen, L. T. Shen, Z. B. Yang, H. Z. Wu, and S. B. Zheng, Enhancement of entanglement in distant mechanical vibrations via modulation in a coupled optomechanical system, *Phys. Rev. A* 89(2), 023843 (2014)
36. X. W. Xu, Y. J. Zhao, and Y. X. Liu, Entangled-state engineering of vibrational modes in a multimembrane optomechanical system, *Phys. Rev. A* 88(2), 022325 (2013)
37. J. Q. Liao, J. F. Huang, and L. Tian, Generation of macroscopic Schrodinger-cat states in qubitoscillator systems, *Phys. Rev. A* 93(3), 033853 (2016)
38. L. Tian, Robust photon entanglement via quantum interference in optomechanical interfaces, *Phys. Rev. Lett.* 110(23), 233602 (2013)
39. Y. D. Wang and A. A. Clerk, Reservoir-engineered entanglement in optomechanical systems, *Phys. Rev. Lett.* 110(25), 253601 (2013)
40. Y. D. Wang, S. Chesi, and A. A. Clerk, Bipartite and tripartite output entanglement in three-mode optomechanical systems, *Phys. Rev. A* 91(1), 013807 (2015)
41. Z. J. Deng, X. B. Yan, Y. D. Wang, and C. W. Wu, Optimizing the output-photon entanglement in multimode optomechanical systems, *Phys. Rev. A* 93(3), 033842 (2016)
42. W. Marshall, C. Simon, R. Penrose, and D. Bouwmeester, Towards quantum superpositions of a mirror, *Phys. Rev. Lett.* 91(13), 130401 (2003)
43. K. Hammerer, M. Wallquist, C. Genes, M. Ludwig, F. Marquardt, P. Treutlein, P. Zoller, J. Ye, and H. J. Kimble, Strong coupling of a mechanical oscillator and a single atom, *Phys. Rev. Lett.* 103(6), 063005 (2009)
44. M. Wallquist, K. Hammerer, P. Zoller, C. Genes, M. Ludwig, F. Marquardt, P. Treutlein, J. Ye, and H. J. Kimble, Single-atom cavity QED and optomicromechanics, *Phys. Rev. A* 81(2), 023816 (2010)
45. J. M. Pirkkalainen, S. U. Cho, F. Massel, J. Tuorila, T. T. Heikkilä, P. J. Hakonen, and M. A. Sillanpää, Cavity optomechanics mediated by a quantum two-level system, *Nat. Commun.* 6(1), 6981 (2015)
46. J. Restrepo, C. Cristiano, and I. Favero, Single-polariton optomechanics, *Phys. Rev. Lett.* 112(1), 013601 (2014)
47. M. Cotrufo, A. Fiore, and E. Verhagen, Coherent atom-phonon interaction through mode field coupling in hybrid optomechanical systems, *Phys. Rev. Lett.* 118(13), 133603 (2017)
48. C. Genes, D. Vitali, and P. Tombesi, Emergence of atom-light-mirror entanglement inside an optical cavity, *Phys. Rev. A* 77, 050307(R) (2008)
49. B. Vogell, K. Stannigel, P. Zoller, K. Hammerer, M. T. Rakher, M. Korppi, A. Jöckel, and P. Treutlein, Cavity-enhanced long-distance coupling of an atomic ensemble to a micromechanical membrane, *Phys. Rev. A* 87(2), 023816 (2013)
50. K. Y. Zhang, L. Zhou, G. Dong, and W. Zhang, Cavity optomechanics with cold atomic gas, *Front. Phys.* 6(3), 237 (2011)
51. Y. Wu, B. Zhu, S.-F Hu, Z. Zhou, and H.-H. Zhong, Floquet control of the gain and loss in a PT-symmetric optical coupler, *Front. Phys.* 12, 121102 (2017)
52. S. Gigan, H. R. Böhm, M. Paternostro, F. Blaser, G. Langer, J. B. Hertzberg, K. C. Schwab, D. Bäuerle, M. Aspelmeyer, and A. Zeilinger, Self-cooling of a micromirror by radiation pressure, *Nature* 444(7115), 67 (2006)
53. O. Arcizet, P. F. Cohadon, T. Briant, M. Pinard, and A. Heidmann, Radiation-pressure cooling and optomechanical instability of a micromirror, *Nature* 444(7115), 71 (2006)
54. I. Wilson-Rae, N. Nooshi, W. Zwerger, and T. J. Kippenberg, Theory of ground state cooling of a mechanical oscillator using dynamical backaction, *Phys. Rev. Lett.* 99(9), 093901 (2007)
55. F. Marquardt, J. P. Chen, A. A. Clerk, and S. M. Girvin, Quantum theory of cavity-assisted sideband cooling of mechanical motion, *Phys. Rev. Lett.* 99(9), 093902 (2007)
56. A. Schliesser, R. Rivi'ere, G. Anetsberger, O. Arcizet, and T. J. Kippenberg, Resolved-sideband cooling of a micromechanical oscillator, *Nat. Phys.* 4(5), 415 (2008)
57. S. Gröblacher, J. B. Hertzberg, M. R. Vanner, G. D. Cole, S. Gigan, K. C. Schwab, and M. Aspelmeyer, Demonstration of an ultracold micro-optomechanical oscillator in a cryogenic cavity, *Nat. Phys.* 5(7), 485 (2009)
58. T. Rocheleau, T. Ndukum, C. Macklin, J. B. Hertzberg, A. A. Clerk, and K. C. Schwab, Preparation and detection of a mechanical resonator near the ground state of motion, *Nature* 463(7277), 72 (2010)

59. A. Schliesser, O. Arcizet, R. Rivi'ere, G. Anetsberger, and T. J. Kippenberg, Resolved-sideband cooling and position measurement of a micromechanical oscillator close to the Heisenberg uncertainty limit, *Nat. Phys.* 5(7), 509 (2009)
60. J. D. Teufel, T. Donner, D. Li, J. W. Harlow, M. S. Allman, K. Cicak, A. J. Sirois, J. D. Whittaker, K. W. Lehnert, and R. W. Simmonds, Sideband cooling of micromechanical motion to the quantum ground state, *Nature* 475(7356), 359 (2011)
61. J. Chan, T. P. M. Alegre, A. H. Safavi-Naeini, J. T. Hill, A. Krause, S. Gröblacher, M. Aspelmeyer, and O. Painter, Laser cooling of a nanomechanical oscillator into its quantum ground state, *Nature* 478(7367), 89 (2011)
62. E. Verhagen, S. Del'eglise, S. Weis, A. Schliesser, and T. J. Kippenberg, Quantum-coherent coupling of a mechanical oscillator to an optical cavity mode, *Nature* 482(7383), 63 (2012)
63. T. J. Kippenberg and K. J. Vahala, Cavity optomechanics: Back-action at the mesoscale, *Science* 321(5893), 1172 (2008)
64. F. Marquardt and S. M. Girvin, Optomechanics, *Physics (College Park Md.)* 2, 40 (2009)
65. X. Wang, H. R. Li, P. B. Li, C. W. Jiang, H. Gao, and F. L. Li, Preparing ground states and squeezed states of nanomechanical cantilevers by fast dissipation, *Phys. Rev. A* 90(1), 013838 (2014)
66. T. Hong, H. Yang, H. Miao, and Y. Chen, Open quantum dynamics of single-photon optomechanical devices, *Phys. Rev. A* 88(2), 023812 (2013)
67. J. Q. Liao, H. K. Cheung, and C. K. Law, Spectrum of single-photon emission and scattering in cavity optomechanics, *Phys. Rev. A* 85(2), 025803 (2012)
68. B. He, Quantum optomechanics beyond linearization, *Phys. Rev. A* 85(6), 063820 (2012)
69. H. Xie, G. W. Lin, X. Chen, Z. H. Chen, and X. M. Lin, Single-photon nonlinearities in a strongly driven optomechanical system with quadratic coupling, *Phys. Rev. A* 93(6), 063860 (2016)
70. X. W. Xu, Y. J. Li, and Y. X. Liu, Photon-induced tunneling in optomechanical systems, *Phys. Rev. A* 87(2), 025803 (2013)
71. A. Kronwald, M. Ludwig, and F. Marquardt, Full photon statistics of a light beam transmitted through an optomechanical system, *Phys. Rev. A* 87(1), 013847 (2013)
72. G. F. Xu and C. K. Law, Dark states of a moving mirror in the single-photon strong-coupling regime, *Phys. Rev. A* 87(5), 053849 (2013)
73. P. Rabl, Photon blockade effect in optomechanical systems, *Phys. Rev. Lett.* 107(6), 063601 (2011)
74. J. Q. Liao and C. K. Law, Correlated two-photon scattering in cavity optomechanics, *Phys. Rev. A* 87(4), 043809 (2013)
75. A. Miranowicz, J. Bajer, N. Lambert, Y. X. Liu, and F. Nori, Tunable multiphonon blockade in coupled nanomechanical resonators, *Phys. Rev. A* 93(1), 013808 (2016)
76. A. Miranowicz, J. Bajer, M. Paprzycka, Y. X. Liu, A. M. Zagoskin, and F. Nori, State-dependent photon blockade via quantum-reservoir engineering, *Phys. Rev. A* 90(3), 033831 (2014)
77. H. Wang, X. Gu, Y. X. Liu, A. Miranowicz, and F. Nori, Tunable photon blockade in a hybrid system consisting of an optomechanical device coupled to a two-level system, *Phys. Rev. A* 92(3), 033806 (2015)
78. D. Leibfried, R. Blatt, C. Monroe, and D. Wineland, Quantum dynamics of single trapped ions, *Rev. Mod. Phys.* 75(1), 281 (2003)
79. J. R. Johansson, P. D. Nation, and F. Nori, Qutip: An open-source Python framework for the dynamics of open quantum systems, *Comput. Phys. Commun.* 183(8), 1760 (2012)
80. J. R. Johansson, P. D. Nation, and F. Nori, QuTiP$_2$: A Python framework for the dynamics of open quantum systems, *Comput. Phys. Commun.* 184(4), 1234 (2013)
81. R. Horodecki, P. Horodecki, M. Horodecki, and K. Horodecki, Quantum entanglement, *Rev. Mod. Phys.* 81(2), 865 (2009)
82. S. B. Zheng and G. C. Guo, Efficient scheme for two-atom entanglement and quantum information processing in cavity QED, *Phys. Rev. Lett.* 85(11), 2392 (2000)
83. W. H. Zurek, Decoherence and the transition from quantum to classical, *Phys. Today* 44(10), 36 (1991)
84. L. F. Buchmann and D. M. Stamper-Kurn, Nondegenerate multimode optomechanics, *Phys. Rev. A* 92(1), 013851 (2015)
85. C. H. Bennett, G. Brassard, C. Cr'epeau, R. Jozsa, A. Peres, and W. K. Wootters, Teleporting an unknown quantum state via dual classical and Einstein-Podolsky-Rosen channels, *Phys. Rev. Lett.* 70(13), 1895 (1993)
86. J. I. Cirac, P. Zoller, H. J. Kimble, and H. Mabuchi, Quantum state transfer and entanglement distribution among distant nodes in a quantum network, *Phys. Rev. Lett.* 78(16), 3221 (1997)